MOLECULAR AND CELLULAR BIOLOGY, Nov. 2007, p. 7727–7734 Vol. 27, No. 21
0270-7306/07/$08.00+0 doi:10.1128/MCB.00959-07

Improved Glucose Homeostasis in Mice with Muscle-Specific Deletion of Protein-Tyrosine Phosphatase 1B▽

Mirela Delibegovic,[1]* Kendra K. Bence,[1]† Nimesh Mody,[2] Eun-Gyoung Hong,[3] Hwi Jin Ko,[3] Jason K. Kim,[3] Barbara B. Kahn,[2]* and Benjamin G. Neel[1]‡

Cancer Biology Program[1] and Division of Endocrinology, Diabetes and Metabolism,[2] Department of Medicine, Beth Israel Deaconess Medical Center and Harvard Medical School, Boston, Massachusetts, and Department of Cellular and Molecular Physiology, Pennsylvania State University College of Medicine, Hershey, Pennsylvania[3]

Received 30 May 2007/Returned for modification 12 July 2007/Accepted 13 August 2007

Obesity and type 2 diabetes are characterized by insulin resistance. Mice lacking the protein-tyrosine phosphatase PTP1B in all tissues are hypersensitive to insulin but also have diminished fat stores. Because adiposity affects insulin sensitivity, the extent to which PTP1B directly regulates glucose homeostasis has been unclear. We report that mice lacking PTP1B only in muscle have body weight and adiposity comparable to those of controls on either chow or a high-fat diet (HFD). Muscle triglycerides and serum adipokines are also affected similarly by HFD in both groups. Nevertheless, muscle-specific PTP1B$^{-/-}$ mice exhibit increased muscle glucose uptake, improved systemic insulin sensitivity, and enhanced glucose tolerance. These findings correlate with and are most likely caused by increased phosphorylation of the insulin receptor and its downstream signaling components. Thus, muscle PTP1B plays a major role in regulating insulin action and glucose homeostasis, independent of adiposity. In addition, rosiglitazone treatment of HFD-fed control and muscle-specific PTP1B$^{-/-}$ mice revealed that rosiglitazone acts additively with PTP1B deletion. Therefore, combining PTP1B inhibition with thiazolidinediones should be more effective than either alone for treating insulin-resistant states.

pType 2 diabetes is a complex disease in which target tissues become resistant to insulin, a phenotype associated with obesity, aging, and a sedentary lifestyle (3). Most actions of insulin are mediated by insulin receptors (IRs) on the plasma membranes of responsive cells (16). Activation of the IR leads to transphosphorylation of tyrosine residues in the IR activation loop, which in turn leads to enhanced ability of the IR to phosphorylate target proteins, such as insulin receptor substrates (IRSs). Tyrosyl-phosphorylated IRS proteins act as docking sites for several SH2 domain-containing proteins, including the p85 regulatory subunit of phosphatidylinositol 3-kinase (PI3K). PI3K becomes activated upon binding to IRS proteins, and its phosphoinositide products facilitate the activation of downstream targets such as Akt, which helps to promote translocation of the glucose transporter GLUT4 from intracellular stores to the cell surface. The detailed mechanism(s) underlying insulin resistance remains controversial (15, 21), but there is general agreement that impaired post-IR signaling is involved (23).

Protein-tyrosine phosphatase 1B (PTP1B) is an abundant, widely expressed nonreceptor tyrosine phosphatase which is thought to be a key negative regulator of insulin signaling (22, 24). Early studies using cultured cells showed that PTP1B overexpression inhibits insulin-stimulated phosphorylation of the IR and IRS-1 (5, 6, 10), whereas introduction of anti-PTP1B antibodies into cells (by osmotic loading) enhances IR signaling (1). Most importantly, global deletion of PTP1B in mice results in increased systemic insulin sensitivity, enhanced glucose uptake into skeletal muscle, and improved glucose tolerance (8, 14). There is also a trend toward decreased hepatic glucose production in PTP1B$^{-/-}$ mice, with no change in glucose uptake in white adipose tissue (WAT) (14). Consistent with these physiological effects, PTP1B$^{-/-}$ mice exhibit enhanced muscle and hepatic IR phosphorylation (8).

These findings implicated PTP1B as an important IR phosphatase in vivo. However, PTP1B$^{-/-}$ mice have decreased body fat on a chow diet and fail to increase their adiposity or body weight when placed on a high-fat diet (HFD) (8, 14). Because adiposity affects insulin sensitivity, it has been difficult to assess the direct role of PTP1B in insulin signaling and glucose homeostasis independent of the body weight/adiposity effects of global PTP1B deficiency.

Antisense oligonucleotides, which reportedly lower PTP1B mRNA and protein levels in liver and fat but not in muscle or brain, normalize blood glucose, improve insulin sensitivity, and attenuate obesity in *ob*/*ob* and *db*/*db* mice (20, 25, 28). These findings suggested that PTP1B may act in liver and/or adipose tissue to regulate glucose homeostasis and adiposity (25). On the other hand, PTP1B levels in muscle are increased in several insulin-resistant states in rodents and humans, and overexpression of PTP1B in muscle alone (27) results in decreased IR signaling in muscle and in systemic insulin resistance. Thus, the site(s) of PTP1B action and its effects on whole-body insulin

* Corresponding author. Present address for Mirela Delibegovic: Zoology Building, Room 311, University of Aberdeen, Tillydrone Avenue, Aberdeen AB24 2TZ, United Kingdom. Phone: 44 1224 273 697. Fax: 44 1224 272 396. E-mail: m.delibegovic@abdn.ac.uk. Mailing address for Barbara B. Kahn: Research North 348, 99 Brookline Ave., Boston, MA 02215. Phone: (617) 667-5422. Fax: (617) 667-2927. E-mail: bkahn@bidmc.harvard.edu.

† Present address: Department of Animal Biology, University of Pennsylvania, School of Veterinary Medicine, Philadelphia, PA.

‡ Present address: Ontario Cancer Institute and Princess Margaret Hospital, Department of Medical Biophysics, University of Toronto, 610 Univ. Ave., Rm. 7-504, Toronto, ON M5G 2M9, Canada.

▽ Published ahead of print on 27 August 2007.

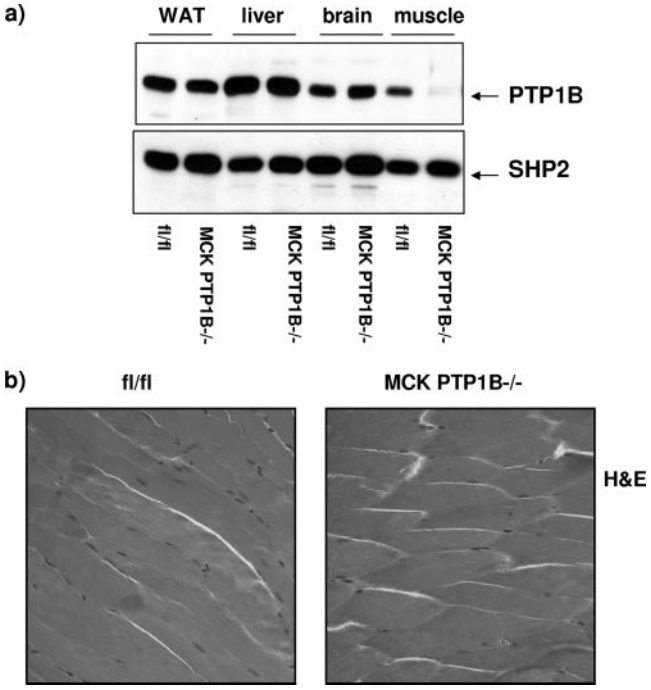

FIG. 1. Muscle-specific PTP1B deletion. (a) Deletion efficiency in the indicated tissues from MCK PTP1B$^{-/-}$ and PTP1B$^{flox/flox}$ littermates. (b) Hematoxylin- and eosin-stained muscles from MCK PTP1B$^{-/-}$ and PTP1B$^{flox/flox}$ littermates.

sensitivity, independent of body mass/adiposity, have remained controversial.

To resolve this controversy, we generated tissue-specific PTP1B knockout mice. We showed recently that only brain-specific deletion of PTP1B protects against diet-induced obesity (2). Muscle or liver-specific PTP1B deletion has no effect on weight gain, whereas adipose PTP1B deficiency increases body weight. Our finding that brain-specific deletion causes weight loss and increased insulin sensitivity raised the possibility that most or even all of the effects of PTP1B deletion in the whole-body knockout were due to lack of PTP1B in the brain rather than to direct effects of PTP1B deficiency on insulin action in the periphery. Because muscle-specific PTP1B$^{-/-}$ mice show no alteration in body weight (2), this allowed us to investigate the role of PTP1B in whole-body glucose homeostasis independently of its effects on body mass and/or adiposity.

MATERIALS AND METHODS

Animal studies. PTP1B-floxed mice were generated as described previously (2). MCK-Cre mice on the FVB background (4) were obtained from C. Ronald Kahn (Joslin Diabetes Center, Boston, MA) and backcrossed to 129-C57BL/6 mice for at least six generations. All mice studied were age-matched littermate males on the mixed Sv129-C57BL/6 background. Mice were maintained on a 12-hour light-dark cycle in a temperature-controlled barrier facility, with free access to water and food (standard Purina lab chow or custom Teklad HFD), as described previously (14). Genotyping was performed by PCR, using DNAs extracted from tail tips (2). Mouse studies were conducted according to federal guidelines and were approved by our Institutional Animal Care and Use Committee.

Body composition. Mice were placed on standard lab chow or HFD at weaning, and weights were monitored weekly for at least 16 weeks. Fat pad weight and carcass analyses were carried out on HFD-fed mice for 18 weeks (14). Carcass

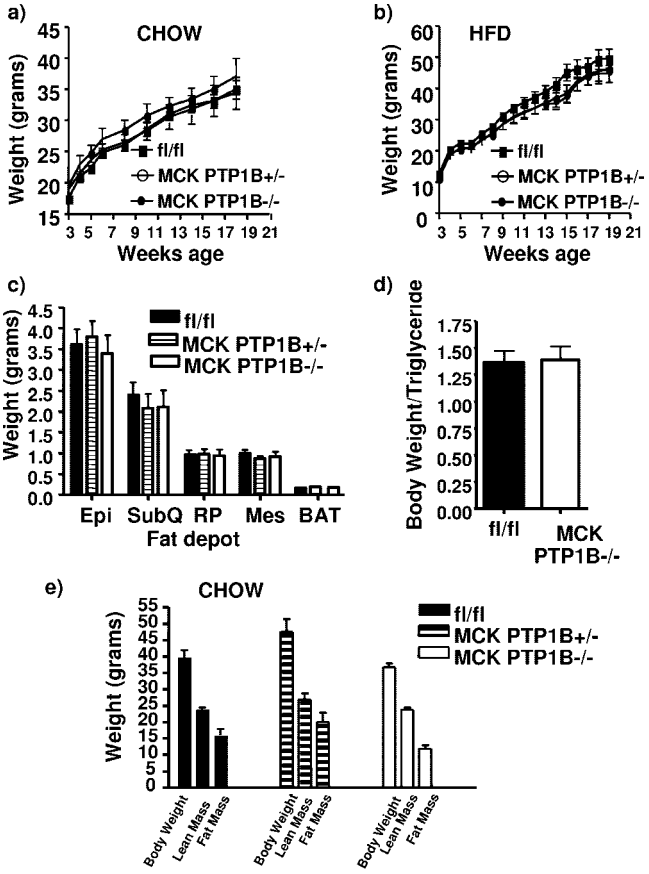

FIG. 2. Muscle-specific PTP1B deletion has no effect on body weight or adiposity. (a) Weight curves for MCK PTP1B$^{-/-}$ ($n = 9$) and PTP1B$^{+/-}$ ($n = 6$) mice versus PTP1B$^{flox/flox}$ controls ($n = 9$) on chow diet. (b) Weight curves for MCK PTP1B$^{-/-}$ ($n = 12$) and PTP1B$^{+/-}$ ($n = 9$) mice versus PTP1B$^{flox/flox}$ controls ($n = 12$) on HFD. The curves show similar results to those we obtained previously (18). (c) Fat pad weights of MCK PTP1B$^{-/-}$ ($n = 12$) and PTP1B$^{+/-}$ ($n = 9$) mice versus PTP1B$^{flox/flox}$ mice ($n = 12$) on HFD. Epi, epididymal; SubQ, subcutaneous; RP, retroperitoneal; Mes, mesenteric; BAT, brown adipose tissue. (d) Total body weight/total body triglyceride ratios from carcass analysis of MCK PTP1B$^{-/-}$ and PTP1B$^{flox/flox}$ mice on HFD. (e) DEXA analysis of MCK PTP1B$^{-/-}$ ($n = 13$), MCK PTP1B$^{+/-}$ ($n = 6$), and PTP1B$^{flox/flox}$ ($n = 14$) mice fed a chow diet. Statistical analysis was performed using two-way ANOVA or one-way ANOVA followed by Tukey's multiple comparison test.

triglycerides were assayed by enzymatic measurement of total and free glycerol concentrations (Sigma triglyceride kit) and were normalized to body weight. Chow-fed mice were subjected to dual-energy X-ray absorptiometry (DEXA) for body composition analysis.

Metabolic measurements. Glucose in tail blood was assayed using a glucometer (One-Touch Basic; Lifescan, Milpitas, CA), with fed measurements taken between 8 and 10 a.m. Where indicated, blood was obtained from mice fasted for 12 h. Serum insulin was determined by enzyme-linked immunosorbent assay (CrystalChem), and free fatty acids (FFAs) were quantified by enzymatic assay (Wako). For insulin tolerance tests (ITTs), 4-h-fasted animals were injected intraperitoneally (i.p.) with 0.75 to 1 mU/g human insulin (HumulinR; Eli Lilly Corp., Indianapolis, IN), and blood glucose values were measured immediately before and 15, 30, 45, 60, 90, and 120 min following injection. For glucose tolerance tests (GTTs), overnight-fasted mice were injected with 20% D-glucose (2 mg/g body weight), and blood glucose was measured immediately before and at 15, 30, 60, and 120 min postinjection. Male mice were 8 and 16 weeks of age at the time of analysis.

Hyperinsulinemic-euglycemic clamps. Two-hour hyperinsulinemic-euglycemic clamps were conducted on awake MCK PTP1B$^{-/-}$ mice ($n = 7$) and

TABLE 1. Metabolic parameters for muscle-specific PTP1B$^{-/-}$ mice[a]

Diet and mouse group	Blood glucose concn (mg/dl)				Serum insulin concn (ng/ml)		Insulin/glucose ratio for fed mice (10^{-7})	Serum FFA concn (mM)	
	Fed 7 wk	Fed 16 wk	Fasted 7 wk	Fasted 16 wk	Fed	Fasted		Fed	Fasted
HFD									
PTP1B$^{flox/flox}$ control	128 ± 7.1	145 ± 3.8	64 ± 3.7	70 ± 6	3.61 ± 0.41	1.03 ± 0.19	39 ± 1	0.46 ± 0.10	0.95 ± 0.24
MCK PTP1B$^{+/-}$	122 ± 6.04	146 ± 12	67 ± 1.7	80 ± 6	2.14 ± 0.5*	0.47 ± 0.08*	23 ± 1*	0.67 ± 0.18	0.77 ± 0.2
MCK PTP1B$^{-/-}$	112 ± 3.53*	130 ± 4*	65 ± 3.5	64 ± 3.7	2.58 ± 0.5*	0.59 ± 0.06*	24 ± 2*	0.37 ± 0.07	0.79 ± 0.16
Chow									
PTP1B$^{flox/flox}$ control	83.5 ± 5.89	94 ± 6	48.5 ± 5.7	58.8 ± 5	0.32 ± 0.07	Not detected	3 ± 0.8	0.36 ± 0.04	ND
MCK PTP1B$^{+/-}$	89.0 ± 5.50	108 ± 8	43.2 ± 2.1	51 ± 4	0.38 ± 0.09	Not detected	3.2 ± 0.7	0.49 ± 0.08	ND
MCK PTP1B$^{-/-}$	75.3 ± 4.53	103 ± 6	42.5 ± 2.7	58.2 ± 1.2	0.26 ± 0.05	Not detected	2.5 ± 0.5	0.31 ± 0.01	ND

[a] Blood glucose, serum insulin, insulin/glucose ratio, and FFAs were analyzed in male PTP1B$^{flox/flox}$ control, MCK PTP1B$^{+/-}$, and MCK PTP1B$^{-/-}$ mice (10 to 15 mice/group) fed HFD or chow, as indicated. Statistical analysis was performed using one-way ANOVA. *, $P < 0.05$ for the indicated genotype compared to flox/flox control littermates. ND, not determined.

PTP1B$^{flox/flox}$ littermates ($n = 5$) at 11 weeks of age (7 weeks on HFD), with a priming dose of insulin (150 mU/kg body weight) followed by a continuous insulin infusion (15 pmol/kg/min). Blood samples (20 μl) were collected at 20-min intervals for the immediate measurement of plasma glucose concentrations, and 20% glucose was infused at variable rates to maintain glucose at basal concentrations. Basal and insulin-stimulated whole-body glucose turnover rates were estimated with a continuous infusion of [3-^{3}H]glucose (Perkin-Elmer Life and Analytical Sciences, Ind., Boston, MA) for 2 h prior to (0.05 mCi/min) and throughout (0.1 mCi/min) the clamps, respectively. All infusions were performed using microdialysis pumps (CMA/Microdialysis, North Chelmsford, MA). To estimate insulin-stimulated glucose uptake in individual tissues, 2-deoxy-D-[1-^{14}C]glucose (2-[^{14}C]DG; Perkin-Elmer Life and Analytical Sciences, Ind.) was administered as a bolus (10 mCi) 75 min after the start of the clamps. Blood samples were taken before, during, and at the end of the clamps for the measurement of plasma [^{3}H]glucose, ^3H_2O, 2-[^{14}C]DG, and/or insulin concentrations. At the end of the clamps, mice were euthanized, and tissues were obtained for biochemical and molecular analysis (11).

Rosiglitazone treatment. Mice fed the HFD for 16 weeks were treated with rosiglitazone by oral gavage. Rosiglitazone (Avandia; GlaxoSmithKline) was powdered with a pestle and mortar and solubilized in 0.5% carboxymethyl cellulose, and mice were treated with 3 μg/g/day. Prior to rosiglitazone treatment, metabolic studies were performed and mice were given 0.5% carboxymethyl cellulose for 10 days in order to get used to oral gavage. Mice were then treated with rosiglitazone for 7 days, and metabolic studies were performed afterwards.

Muscle and heart triglyceride assay. Muscles and hearts were weighed, ground in liquid N_2, and placed in polypropylene tubes. Phosphate-buffered saline (PBS) (2 ml) was added to each tube, and the samples were homogenized further. Two milliliters of chloroform-methanol (2:1) was added, and the tubes were vortexed and centrifuged for 30 min at 3,500 rpm. The bottom layer was removed, and 100 μl was added to test tubes, dried under nitrogen gas, and resuspended in 100 μl of PBS containing 1% Triton X-100. One milliliter of triglyceride analysis solution (Sigma) was added to the tubes, which included the blank and standards provided with the kit. After incubation at room temperature for 15 min, the A_{540} was measured, and triglycerides were quantified by reference to a standard curve.

Biochemical analysis. Mouse tissues were dissected and immediately frozen in liquid N_2. Whole-cell lysates were prepared by extraction in radioimmunoprecipitation assay buffer (10 mM Tris-HCl, pH 7.4, 150 mM NaCl, 0.1% sodium dodecyl sulfate [SDS], 1% Triton X-100, 1% sodium deoxycholate, 5 mM EDTA, 1 mM NaF, 1 mM sodium orthovanadate, protease inhibitors) at 4°C, followed by clarification at 14,000 × *g* (27). Proteins were resolved by SDS-polyacrylamide gel electrophoresis and transferred to nitrocellulose membranes. Immunoblots were performed with anti-phosphotyrosine monoclonal antibody 4G10 (Upstate Biotechnology) or with polyclonal antibodies against the IRβ subunit (Santa Cruz), IRS-1 (gift of M. White, Joslin Diabetes Center), pIRS1 S307, S612, and S636 (Cell Signaling), extracellular signal-regulated kinase 1/2 or SHP2 (Santa Cruz), pAkt, Akt, glycogen synthase kinase 3 (Cell Signaling), or PTP1B (Upstate Biotechnology), following the manufacturer's directions. Proteins were visualized with fluorescent secondary antibodies and quantified with an Odyssey infrared imaging system (LI-COR Biosciences, Lincoln, NE) or by enhanced chemiluminescence followed by densitometry (Molecular Dynamics/Amersham Biosciences Corp.). For insulin signaling experiments, animals were fasted overnight for 12 h, injected i.p. with insulin (10 mU/g body weight), and sacrificed 10 min later. Tissues were dissected and snap-frozen in liquid N_2. Muscle lysates were prepared as described above, and proteins (500 μg) were subjected to immunoprecipitation with anti-IRβ or anti-IRS-1 (3 μl) antibodies, as described above. Immune complexes were collected on protein A-Sepharose beads (Sigma, St. Louis, MO), washed three times with lysis buffer and twice with 1× PBS (Gibco-BRL, Gaithersburg, MD) containing 2 mM Na_3VO_4, resuspended in

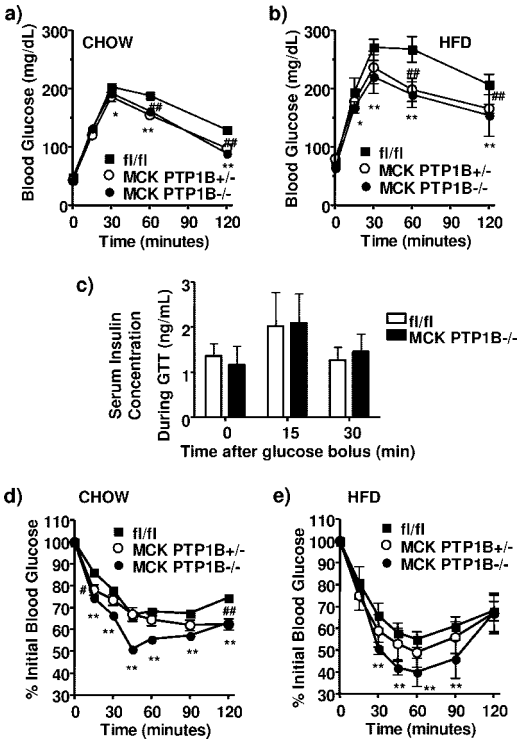

FIG. 3. Improved insulin sensitivity and glucose homeostasis in MCK PTP1B$^{-/-}$ mice. (a) GTT results for male MCK PTP1B$^{-/-}$ ($n = 12$), MCK PTP1B$^{+/-}$ ($n = 6$), and PTP1B$^{flox/flox}$ control ($n = 14$) mice on chow diet. (b) GTT results for male MCK PTP1B$^{-/-}$ ($n = 12$), MCK PTP1B$^{+/-}$ ($n = 9$), and PTP1B$^{flox/flox}$ ($n = 12$) mice on HFD. (c) Insulin concentrations during GTTs in male MCK PTP1B$^{-/-}$ ($n = 4$) and PTP1B$^{flox/flox}$ ($n = 6$) mice on HFD. (d) ITT results for male MCK PTP1B$^{-/-}$ ($n = 12$), MCK PTP1B$^{+/-}$ ($n = 6$), and PTP1B$^{flox/flox}$ ($n = 14$) mice on chow (insulin dose, 0.75 mU/g). (e) ITT results for male MCK PTP1B$^{-/-}$ ($n = 12$), MCK PTP1B$^{+/-}$ ($n = 9$), and PTP1B$^{flox/flox}$ ($n = 12$) mice on HFD (insulin dose, 1 mU/g). Statistical analysis was performed using two-way ANOVA (**, $P < 0.01$; *, $P < 0.05$ [for MCK PTP1B$^{-/-}$ versus PTP1B$^{flox/flox}$ mice]; ##, $P < 0.01$; #, $P < 0.05$ [for MCK PTP1B$^{+/-}$ versus PTP1B$^{flox/flox}$ mice]).

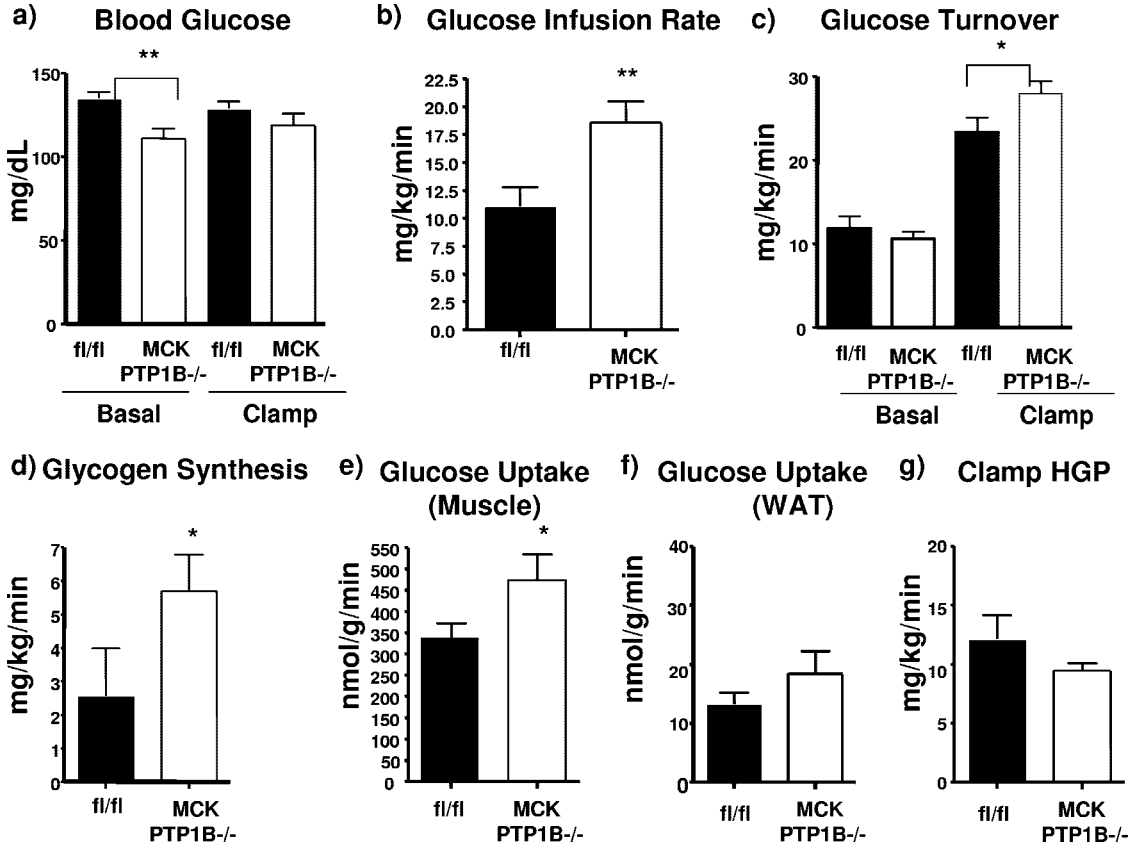

FIG. 4. Glucose metabolism as measured by hyperinsulinemic-euglycemic clamp studies. (a) Basal and clamp glucose levels in MCK PTP1B$^{-/-}$ (n = 7) and PTP1B$^{flox/flox}$ control (n = 5) mice on HFD for 7 weeks. (b) Whole-body glucose infusion rates. (c) Glucose turnover rates. (d) Glycogen synthesis rates. (e) Glucose uptake into gastrocnemius muscle. (f) Glucose uptake into WAT. (g) Hepatic glucose production. The data shown in panels b to f were all measured during the clamp. Results are means with SEM, and statistical analysis was performed using one-tailed Student's t test (**, $P < 0.01$; *, $P < 0.05$).

SDS-polyacrylamide gel electrophoresis sample buffer, and heated for 10 min at 95°C. For PI3K assays, tissue lysates (500 μg protein) were subjected to immunoprecipitation with IRS-1 antibodies (1:100 dilution), and PI3K activity in immune complexes was assessed as described previously (13).

Statistical analysis. Results are expressed as means ± standard errors of the means (SEM). Comparisons between groups were made by unpaired two-tailed Student's t test, one-way analysis of variance (ANOVA), or two-way ANOVA, as appropriate, with P values of <0.05 considered statistically significant.

RESULTS

Generation of mice with muscle-specific deletion of PTP1B and its effects on body mass and adiposity. Mice with a muscle-specific deletion of PTP1B were generated by crossing PTP1B$^{flox/flox}$ mice to mice expressing Cre recombinase under the control of the muscle creatine kinase promoter enhancer (MCK-Cre), thereby generating MCK PTP1B$^{+/flox}$ mice (2). These mice were crossed to PTP1B$^{flox/flox}$ mice to yield MCK PTP1B$^{flox/flox}$ mice, which lack PTP1B in skeletal muscle (hereafter termed MCK PTP1B$^{-/-}$ mice) but not in other insulin-responsive tissues (Fig. 1a). Hematoxylin and eosin staining of muscle sections revealed no differences in histology between MCK PTP1B$^{-/-}$ and PTP1B$^{flox/flox}$ control littermates (Fig. 1b), and muscle glycogen contents were also the same (data not shown).

MCK PTP1B$^{-/-}$ mice were weaned onto either HFD (55% fat by weight) or normal chow diet (4.5% fat by weight). As expected from previous studies (2), MCK PTP1B$^{-/-}$ mice and PTP1B$^{flox/flox}$ littermate controls showed comparable body masses on chow and HFD (Fig. 2a and b). Adiposity, as assessed by fat pad weights (Fig. 2c), total body carcass triglyceride content (Fig. 2d), or DEXA analysis (Fig. 2e), also was similar in both groups. In addition, serum FFAs were unchanged on the HFD and chow diet in both the fed and fasted states (Table 1).

Improved glucose homeostasis in muscle-specific PTP1B knockout mice. In spite of their similar body weights and adiposity, fed glucose levels in MCK PTP1B$^{-/-}$ mice on HFD were lower than those in control littermates (Table 1). MCK PTP1B$^{-/-}$ mice on either HFD or chow also had a considerably enhanced ability to clear glucose from the peripheral circulation during i.p. GTTs (Fig. 3a and b). There was no difference in insulin secretion between MCK PTP1B$^{-/-}$ mice and control littermates during the first 30 min of the GTT (Fig. 3c), suggesting that the improvement in glucose homeostasis was due to improved insulin sensitivity. Consistent with this conclusion, circulating insulin levels in MCK PTP1B$^{-/-}$ mice on HFD were decreased ~30% in the fed state, and the insulin/glucose ratio was decreased ~40% (Table 1). In the fasted state, circulating insulin levels in MCK PTP1B$^{-/-}$ mice on HFD were decreased ~45%. MCK PTP1B$^{-/-}$ mice also

showed a significantly greater decrease in blood glucose during ITTs (Fig. 3d and e) on either chow or HFD. Even mice with only a 50% reduction of PTP1B levels in muscle (MCK PTP1B$^{+/-}$ mice) exhibited improved glucose homeostasis, as revealed by enhanced glucose tolerance on both diets (Fig. 3a and b) and lower fed and fasted insulin levels and insulin/glucose ratios on HFD (Table 1). Thus, selective PTP1B deficiency in muscle increases systemic insulin sensitivity without altering adiposity.

Increased muscle glucose uptake in muscle-specific PTP1B knockout mice. To determine which tissues are involved in the effects of muscle PTP1B deficiency on glucose utilization, we performed hyperinsulinemic-euglycemic clamp studies on MCK PTP1B$^{-/-}$ and PTP1B$^{flox/flox}$ control mice maintained on HFD for 7 weeks. Consistent with our findings with other litters of mice (Table 1), basal blood glucose levels in MCK PTP1B$^{-/-}$ mice were lower than those in control littermates and were maintained at levels comparable to those of controls during the clamp (Fig. 4a). However, the glucose infusion rate required to maintain euglycemia in the presence of a constant infusion of insulin was 40% higher for MCK PTP1B$^{-/-}$ mice than for control littermates (Fig. 4b), an increase comparable to that seen for whole-body PTP1B$^{-/-}$ mice (14). The glucose turnover rate and glycogen synthesis were also increased in MCK PTP1B$^{-/-}$ mice (Fig. 4c and d). Glucose uptake into skeletal muscle was 40% higher in MCK PTP1B$^{-/-}$ mice than in controls (Fig. 4e), whereas glucose uptake into WAT (Fig. 4f) and hepatic glucose production (Fig. 4g) were unaffected by PTP1B deficiency in muscle.

Increased insulin signaling in muscle-specific PTP1B knockout mice. To investigate the molecular mechanism of increased insulin sensitivity in MCK PTP1B$^{-/-}$ mice, we injected the mice with insulin or saline (control) and analyzed insulin signaling components in muscles from these mice. In muscles from MCK PTP1B$^{-/-}$ mice (on chow), the IR was basally hyperphosphorylated to levels comparable to those seen following insulin stimulation of control mice, which presumably represents maximal IR phosphorylation (Fig. 5a and f). There also was basal IR hyperphosphorylation (compared to controls) in muscles from MCK PTP1B$^{-/-}$ mice maintained on HFD (Fig. 5b and f). High-fat feeding diminishes insulin sensitivity, resulting in a smaller increase in IR phosphorylation in HFD-fed than in chow-fed control (flox/flox) mice. Muscle PTP1B deficiency overcomes these effects of HFD, as insulin-induced IR phosphorylation in MCK PTP1B$^{-/-}$ muscle was higher than that in controls (Fig. 5b). Basal and insulin-stimulated IRS1 phosphorylation was also higher in MCK PTP1B$^{-/-}$ mice on HFD (Fig. 5c and f), as was insulin-stimulated IRS1-associated PI3K activity (Fig. 5d) and Akt phosphorylation (Fig. 5e). Basal phosphorylation of Erk1/2 was also higher in MCK PTP1B$^{-/-}$ mice, further suggesting that insulin signaling is increased in these mice (Fig. 5e). The absence of basal activation of PI3K and Akt is probably due to compensatory actions of other phosphatases, such as PTEN or SHIP-2. We did not observe increased insulin signaling in other tissues, such as the liver. These biochemical data strongly suggest that improved whole-body glucose homeostasis in MCK PTP1B$^{-/-}$ mice is the direct result of increased insulin signaling and glucose uptake in muscle.

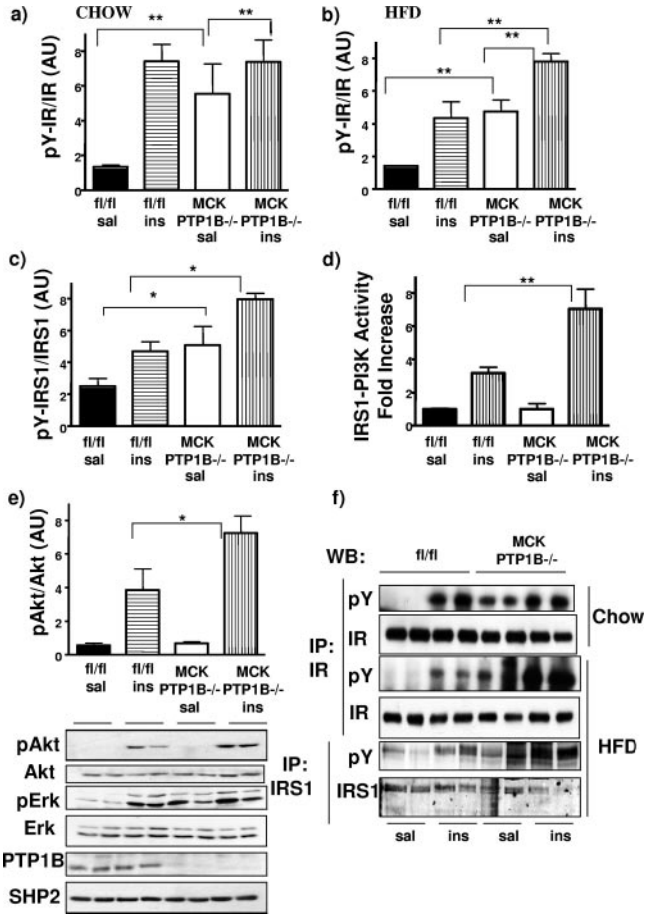

FIG. 5. Enhanced insulin sensitivity in MCK PTP1B$^{-/-}$ mice. (a and b) IR phosphorylation in muscles from mice fed with chow (a) or HFD (b) and injected with saline or insulin (10 mU/g i.p.). Lysates were immunoprecipitated with IR antibodies, immunoblotted with anti-phosphotyrosine antibody, and then stripped and reprobed with IR antibodies to control for loading. Immunoblots were then quantified using an Odyssey infrared imaging system. Bar graphs represent pooled, normalized data (arbitrary units) for MCK PTP1B$^{-/-}$ (n = 4 and 6 [for saline and insulin groups, respectively]) and PTP1B$^{flox/flox}$ (n = 4 and 6) mice (males; 18 weeks on each diet). (c) IRS1 tyrosine phosphorylation in muscles from HFD-fed MCK PTP1B$^{-/-}$ mice (n = 4 and 6) and PTP1B$^{flox/flox}$ controls (n = 4 and 6). Lysates were immunoprecipitated with IRS1 antibodies, immunoblotted with anti-phosphotyrosine antibody, and then stripped and reprobed with IRS1 antibodies to control for loading. Immunoblots were then quantified using an Odyssey infrared imaging system. (d) IRS1-associated PI3K activity, expressed as x-fold increases from basal activity, in muscles from HFD-fed MCK PTP1B$^{-/-}$ (n = 3 and 6) and PTP1B$^{flox/flox}$ (n = 3 and 6) mice. There was no difference in basal PI3K activity between MCK PTP1B$^{-/-}$ and PTP1B$^{flox/flox}$ mice. (e) Akt phosphorylation, as assessed by immunoblots, in muscle lysates from HFD-fed MCK PTP1B$^{-/-}$ (n = 4 and 4) and PTP1B$^{flox/flox}$ (n = 4 and 4) mice. A representative blot is shown, wherein each lane represents the muscle lysate from a different mouse. The blot was reprobed with anti-PTP1B antibodies to show the absence of PTP1B in muscles of MCK PTP1B$^{-/-}$ mice. Proteins were visualized by enhanced chemiluminescence, and the data were pooled, normalized, and represented in a bar graph. (f) Representative blots of IR phosphorylation in muscle lysates from mice on chow and HFD, as well as IRS1 phosphorylation. Statistical analysis was performed using one-way ANOVA followed by Tukey's multiple comparison test (**, $P < 0.01$; *, $P < 0.05$).

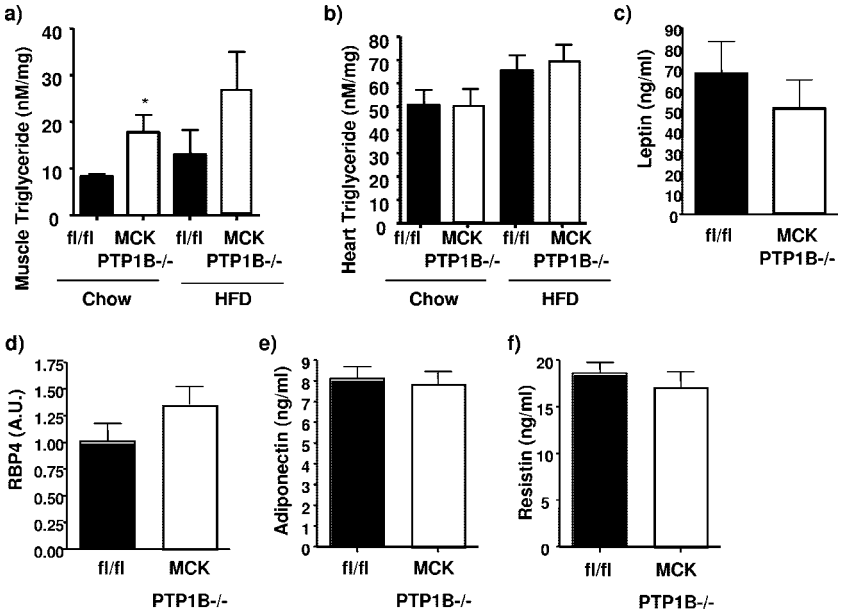

FIG. 6. Tissue triglycerides and adipokine levels in MCK PTP1B$^{-/-}$ and PTP1B$^{flox/flox}$ control mice. (a) Muscle triglycerides in MCK PTP1B$^{-/-}$ ($n = 6$) and PTP1B$^{flox/flox}$ control ($n = 6$) mice on chow and in MCK PTP1B$^{-/-}$ ($n = 5$) and PTP1B$^{flox/flox}$ control ($n = 5$) mice on HFD. (b) Heart triglycerides in MCK PTP1B$^{-/-}$ ($n = 6$) and PTP1B$^{flox/flox}$ control ($n = 6$) mice on chow and in MCK PTP1B$^{-/-}$ ($n = 5$) and PTP1B$^{flox/flox}$ control ($n = 5$) mice on HFD. Serum leptin (c), RBP4 (d), adiponectin (e), and resistin (f) levels in MCK PTP1B$^{-/-}$ ($n = 8$) and PTP1B$^{flox/flox}$ control ($n = 8$) mice on HFD were also measured. Results are means with SEM, and statistical analysis was performed using one-tailed Student's t test (*, $P < 0.05$).

Improved insulin sensitivity in MCK PTP1B$^{-/-}$ mice is independent of changes in tissue triglycerides and/or adipokines. Muscle triglycerides have been reported to be important in the etiology of insulin resistance (21). We measured the levels of muscle triglycerides in our mice on both chow and HFD. MCK PTP1B$^{-/-}$ mice actually had higher skeletal muscle triglycerides than their control littermates on the chow diet (Fig. 6a). As expected, high-fat feeding increased muscle triglycerides further, with muscle triglycerides still tending to be higher in MCK PTP1B$^{-/-}$ mice than in controls (Fig. 6a). Heart triglycerides were unchanged in both groups of mice (Fig. 6b). It has been hypothesized previously that intracellular fatty acid metabolites activate a serine kinase cascade that results in increased phosphorylation of IRS1 on critical serine residues (17). We assessed serine phosphorylation of these sites (IRS1 S307, S612, and S636) and found it to be unchanged between MCK PTP1B$^{-/-}$ mice and PTP1B$^{flox/flox}$ control littermates (data not shown). Serum leptin, RBP4, adiponectin, and resistin levels were similar in MCK PTP1B$^{-/-}$ mice and PTP1B$^{flox/flox}$ control mice (Fig. 6c to f).

Rosiglitazone treatment of muscle-specific PTP1B$^{-/-}$ mice. Thiazolidinediones such as rosiglitazone are agonists of the nuclear hormone receptor peroxisome proliferator-activated receptor γ (PPARγ) and are widely used in the treatment of type 2 diabetes. PPARγ agonists improve muscle glucose uptake, and treatment of HFD-fed, streptozotocin-treated diabetic rats with rosiglitazone results in decreased muscle PTP1B levels (26). High-fat feeding increases levels of muscle PTP1B in mice (data not shown), raising the possibility that the antidiabetic effects of rosiglitazone involve decreasing muscle PTP1B levels.

To investigate this possibility, we assessed the effects of rosiglitazone on HFD-fed MCK PTP1B$^{-/-}$ mice and PTP1B$^{flox/flox}$ control littermates. As expected, MCK PTP1B$^{-/-}$ mice exhibited improved glucose tolerance in comparison to that of their PTP1B$^{flox/flox}$ control littermates prior to rosiglitazone treatment (Fig. 7a). Rosiglitazone improved glucose tolerance in PTP1B$^{flox/flox}$ controls and further improved glucose tolerance in MCK PTP1B$^{-/-}$ mice (Fig. 7a). Insulin sensitivity, which is markedly improved in MCK PTP1B$^{-/-}$ mice prior to rosiglitazone treatment (Fig. 7b), was also further improved following drug treatment (Fig. 7b). Blood glucose and insulin levels were improved in both genotypes of mice following rosiglitazone treatment (Fig. 7c). Therefore, rosiglitazone treatment had an additive effect with muscle PTP1B deletion to improve glucose homeostasis and insulin sensitivity.

DISCUSSION

We generated mice with muscle-specific PTP1B deletion to ascertain the role of muscle PTP1B in body mass regulation and glucose homeostasis. As reported previously, MCK PTP1B$^{-/-}$ mice weigh the same as their control PTP1B$^{flox/flox}$ littermates on HFD. Furthermore, we show here that there are no weight differences on a chow diet and that muscle-specific PTP1B deletion does not affect adiposity, as measured by fat pad weight, total body carcass analysis, and DEXA analysis of the mice.

Nevertheless, despite the absence of any differences in body weight and/or adiposity, MCK PTP1B$^{-/-}$ mice exhibit marked improvements in whole-body glucose homeostasis and insulin sensitivity, as evidenced by a considerably enhanced ability to clear glucose from the peripheral circulation during i.p. glucose tolerance tests and a significantly greater decrease in

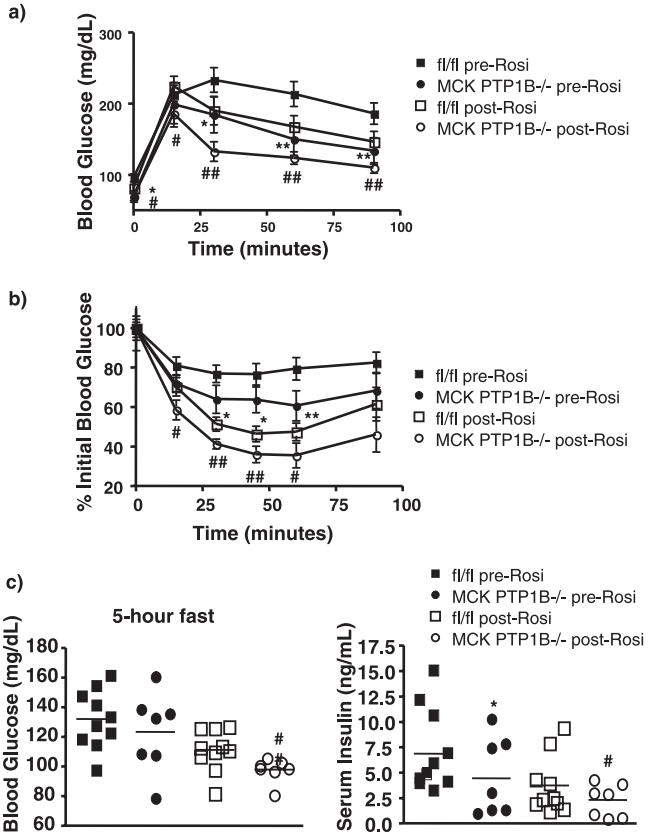

FIG. 7. Rosiglitazone treatment leads to improved insulin sensitivity and glucose homeostasis in MCK PTP1B$^{-/-}$ mice. (a) GTT results for male MCK PTP1B$^{-/-}$ (n = 7; filled circles) and PTP1B$^{flox/flox}$ control (n = 10; filled squares) mice on HFD prior to rosiglitazone treatment and for MCK PTP1B$^{-/-}$ (n = 7; empty circles) and PTP1B$^{flox/flox}$ (n = 10; empty squares) mice on HFD after rosiglitazone treatment. (b) ITT results for male MCK PTP1B$^{-/-}$ (n = 7; filled circles) and PTP1B$^{flox/flox}$ (n = 10; filled squares) mice on HFD prior to rosiglitazone treatment (insulin dose, 1.2 mU/g) and for MCK PTP1B$^{-/-}$ (n = 7; empty circles) and PTP1B$^{flox/flox}$ (n = 10; empty squares) mice on HFD after rosiglitazone treatment (insulin dose, 1.2 mU/g). (c) Fasted (5 h) blood glucose and serum insulin levels before and after rosiglitazone treatment. Statistical analysis was performed using two-way ANOVA (**, $P < 0.01$; *, $P < 0.05$ [for MCK PTP1B$^{-/-}$ versus PTP1B$^{flox/flox}$ mice, both prior to rosiglitazone treatment]; ##, $P < 0.01$; #, $P < 0.05$ [for MCK PTP1B$^{-/-}$ versus PTP1B$^{flox/flox}$ mice, both after rosiglitazone treatment]).

blood glucose during insulin tolerance tests. Thus, selective PTP1B deficiency in muscle increases systemic insulin sensitivity in the absence of changes in adiposity.

Hyperinsulinemic-euglycemic clamp studies showed a comparable increase in insulin sensitivity in MCK PTP1B$^{-/-}$ mice to that seen in whole-body PTP1B$^{-/-}$ mice (14). This was due to increased glucose uptake into skeletal muscle, which was 40% higher in MCK PTP1B$^{-/-}$ mice than in control mice. These data indicate that a lack of PTP1B in muscle is a major cause of the increase in whole-body insulin sensitivity and glucose handling in whole-body PTP1B$^{-/-}$ mice under clamp conditions (hyperinsulinemia). Under euglycemic conditions or during fasting, PTP1B deficiency in the liver may also contribute to improved insulin sensitivity in whole-body PTP1B$^{-/-}$ mice. Indeed, preliminary studies of liver-specific PTP1B$^{-/-}$ mice are consistent with this notion (M. Delibegovic, B. B. Kahn, B. G. Neel, and K. Bence, unpublished observations). Furthermore, we showed previously that young female mice with a brain-specific deletion of PTP1B have similar body masses to those of control mice yet also exhibit improved glucose homeostasis (2). Indeed, neuronal PTP1B may regulate systemic insulin sensitivity in the absence of changes in adiposity, although we did not assess body fat content in female brain-specific knockout mice at this young age. In any case, the results herein show unambiguously that muscle PTP1B is an important regulator of insulin sensitivity independent of body weight/adiposity.

Although PTP1B is known to be an IR phosphatase, in vitro studies indicate that it can also dephosphorylate IRS1. Here we show that the IR and IRS1 are basally hyperphosphorylated in muscles from MCK PTP1B$^{-/-}$ mice to levels comparable to those seen following insulin stimulation of control mice. Insulin-stimulated phosphorylation of the signaling components downstream of IRS1 is also higher in muscles from MCK PTP1B$^{-/-}$ mice. Thus, our biochemical data support the notion that improved whole-body glucose homeostasis in MCK PTP1B$^{-/-}$ mice is the direct result of increased insulin signaling and glucose uptake in muscle.

Among the major (although not mutually exclusive) models currently proposed for the pathogenesis of insulin resistance, one proposes that increased tissue triglyceride content causes insulin resistance (21), whereas another implicates differences in serum adipokine levels (15). MCK PTP1B$^{-/-}$ mice actually had higher skeletal muscle triglycerides than their control littermates on a chow diet. As expected, high-fat feeding increased muscle triglycerides further, with muscle triglycerides still tending to be higher in MCK PTP1B$^{-/-}$ mice than in controls. Increased muscle triglyceride accumulation may be due to increased glucose uptake into the muscle. Furthermore, serum adiponectin, leptin, resistin, and RBP4 levels were similar in MCK PTP1B$^{-/-}$ mice and PTP1B$^{flox/flox}$ controls. With all else being equal, the increased muscle fat in MCK PTP1B$^{-/-}$ mice compared to that in controls and a lack of improvement in the serum adipokine profile would be expected to impair muscle insulin responsiveness. Yet in marked contrast to this expectation, PTP1B deficiency in muscle improves insulin sensitivity and rescues insulin resistance on HFD. Thus, PTP1B deficiency is able to bypass the two major pathogenic mechanisms currently proposed for insulin resistance.

The role of muscle in whole-body glucose homeostasis has been controversial. Muscle-specific IR knockout mice develop insulin resistance in muscle and have increased adiposity (4) yet remain normoglycemic, most likely because of increased glucose uptake into WAT (7, 12) and/or the effects of increased serum adiponectin levels (7). On the other hand, the phenotypes of mice expressing dominant-negative *Igf1r* or with muscle-specific knockout of *Glut4* indicate a key role for muscle glucose uptake in systemic glucose homeostasis (9, 18, 29). The effects of muscle PTP1B deficiency show that increasing insulin-stimulated glucose uptake into muscle alone is sufficient to improve systemic insulin sensitivity and restore normal glucose homeostasis in mice with obesity caused by high-fat feeding. Furthermore, muscle PTP1B overexpression decreases glucose uptake into the muscle and results in insulin resistance (17).

Our findings have several potentially important therapeutic implications. In view of the salutary effects of PTP1B deficiency on body mass and glucose homeostasis, several pharmaceutical companies are attempting to develop PTP1B inhibitors for the treatment of diabetes and/or obesity. The design of such agents has proved challenging, with the most active compounds tending to be highly charged and unlikely to gain access to the central nervous system (19). Although our previous studies showed that inhibiting neuronal PTP1B is critical for conferring the beneficial effects of PTP1B deficiency on body mass/adiposity (2), our current results indicate that even agents that inhibit PTP1B only in peripheral tissues should improve insulin sensitivity and systemic glucose homeostasis substantially. Moreover, PPARγ agonists improve muscle glucose uptake, and treatment of HFD-fed, streptozotocin-treated diabetic rats with the PPARγ agonist rosiglitazone results in decreased muscle PTP1B levels (26). Our data suggest that rosiglitazone treatment has dramatic effects on glucose homeostasis in mice with a muscle-specific deletion of PTP1B, thus suggesting that rosiglitazone could be added to PTP1B inhibitors in order to alleviate the diabetic phenotype caused by high-fat feeding.

ACKNOWLEDGMENTS

We thank C. Ronald Kahn (Joslin Diabetes Center) for MCK-Cre mice, Young-Bum Kim (BIDMC) for helpful advice on PI3K assays, and Odile Peroni and Thomas Pulinilkunnil (BIDMC) for helpful advice regarding rosiglitazone experiment.

This work was supported by NIH grants DK 60838 and R37 49132 (B.G.N.) and DK 60839 (B.B.K.), by Physiology Core grant DK57521 (B.B.K.), and by a research grant from the American Diabetes Association (B.G.N.). M.D. is the recipient of a postdoctoral fellowship from the American Heart Association. K.K.B. was supported by a postdoctoral fellowship from the Charles A. King Trust (The Medical Foundation) and by a pilot and feasibility grant from the Boston Obesity and Nutrition Research Center (5-P30-DK046200). N.M. is the recipient of a postdoctoral fellowship from the European Association for the Study of Diabetes (EASD) and the American Diabetes Association. Part of this study was performed at the Penn State Mouse Metabolic Phenotyping Center and was supported by grants from the American Diabetes Association (1-04-RA-47 to J.K.K.) and the Pennsylvania Department of Health (Tobacco Settlement Award to J.K.K.).

REFERENCES

1. **Ahmad, F., and B. J. Goldstein.** 1995. Increased abundance of specific skeletal muscle protein-tyrosine phosphatases in a genetic model of insulin-resistant obesity and diabetes mellitus. Metabolism **44:**1175–1184.
2. **Bence, K. K., M. Delibegovic, B. Xue, C. Z. Gorgun, G. S. Hotamisligil, B. G. Neel, and B. B. Kahn.** 2006. Neuronal PTP1B regulates body weight, adiposity and leptin action. Nat. Med. **12:**917–924.
3. **Biddinger, S. B., and C. R. Kahn.** 2006. From mice to men: insights into the insulin resistance syndromes. Annu. Rev. Physiol. **68:**123–158.
4. **Bruning, J. C., M. D. Michael, J. N. Winnay, T. Hayashi, D. Horsch, D. Accili, L. J. Goodyear, and C. R. Kahn.** 1998. A muscle-specific insulin receptor knockout exhibits features of the metabolic syndrome of NIDDM without altering glucose tolerance. Mol. Cell **2:**559–569.
5. **Byon, J. C., K. A. Kenner, A. B. Kusari, and J. Kusari.** 1997. Regulation of growth factor-induced signaling by protein-tyrosine-phosphatases. Proc. Soc. Exp. Biol. Med. **216:**1–20.
6. **Byon, J. C., A. B. Kusari, and J. Kusari.** 1998. Protein-tyrosine phosphatase-1B acts as a negative regulator of insulin signal transduction. Mol. Cell. Biochem. **182:**101–108.
7. **Cariou, B., C. Postic, P. Boudou, R. Burcelin, C. R. Kahn, J. Girard, A. F. Burnol, and F. Mauvais-Jarvis.** 2004. Cellular and molecular mechanisms of adipose tissue plasticity in muscle insulin receptor knockout mice. Endocrinology **145:**1926–1932.
8. **Elchebly, M., P. Payette, E. Michaliszyn, W. Cromlish, S. Collins, A. L. Loy, D. Normandin, A. Cheng, J. Himms-Hagen, C. C. Chan, C. Ramachandran, M. J. Gresser, M. L. Tremblay, and B. P. Kennedy.** 1999. Increased insulin sensitivity and obesity resistance in mice lacking the protein tyrosine phosphatase-1B gene. Science **283:**1544–1548.
9. **Fernandez, A. M., J. K. Kim, S. Yakar, J. Dupont, C. Hernandez-Sanchez, A. L. Castle, J. Filmore, G. I. Shulman, and D. Le Roith.** 2001. Functional inactivation of the IGF-I and insulin receptors in skeletal muscle causes type 2 diabetes. Genes Dev. **15:**1926–1934.
10. **Kenner, K. A., E. Anyanwu, J. M. Olefsky, and J. Kusari.** 1996. Protein-tyrosine phosphatase 1B is a negative regulator of insulin- and insulin-like growth factor-I-stimulated signaling. J. Biol. Chem. **271:**19810–19816.
11. **Kim, H. J., T. Higashimori, S. Y. Park, H. Choi, J. Dong, Y. J. Kim, H. L. Noh, Y. R. Cho, G. Cline, Y. B. Kim, and J. K. Kim.** 2004. Differential effects of interleukin-6 and -10 on skeletal muscle and liver insulin action in vivo. Diabetes **53:**1060–1067.
12. **Kim, J. K., M. D. Michael, S. F. Previs, O. D. Peroni, F. Mauvais-Jarvis, S. Neschen, B. B. Kahn, C. R. Kahn, and G. I. Shulman.** 2000. Redistribution of substrates to adipose tissue promotes obesity in mice with selective insulin resistance in muscle. J. Clin. Investig. **105:**1791–1797.
13. **Kim, Y. B., S. E. Nikoulina, T. P. Ciaraldi, R. R. Henry, and B. B. Kahn.** 1999. Normal insulin-dependent activation of Akt/protein kinase B, with diminished activation of phosphoinositide 3-kinase, in muscle in type 2 diabetes. J. Clin. Investig. **104:**733–741.
14. **Klaman, L. D., O. Boss, O. D. Peroni, J. K. Kim, J. L. Martino, J. M. Zabolotny, N. Moghal, M. Lubkin, Y. B. Kim, A. H. Sharpe, A. Stricker-Krongrad, G. I. Shulman, B. G. Neel, and B. B. Kahn.** 2000. Increased energy expenditure, decreased adiposity, and tissue-specific insulin sensitivity in protein-tyrosine phosphatase 1B-deficient mice. Mol. Cell. Biol. **20:**5479–5489.
15. **Kobayashi, K.** 2005. Adipokines: therapeutic targets for metabolic syndrome. Curr. Drug Targets **6:**525–529.
16. **Lizcano, J. M., and D. R. Alessi.** 2002. The insulin signalling pathway. Curr. Biol. **12:**R236–R238.
17. **Morino, K., K. F. Petersen, S. Dufour, D. Befroy, J. Frattini, N. Shatzkes, S. Neschen, M. F. White, S. Bilz, S. Sono, M. Pypaert, and G. I. Shulman.** 2005. Reduced mitochondrial density and increased IRS-1 serine phosphorylation in muscle of insulin-resistant offspring of type 2 diabetic parents. J. Clin. Investig. **115:**3587–3593.
18. **Nandi, A., Y. Kitamura, C. R. Kahn, and D. Accili.** 2004. Mouse models of insulin resistance. Physiol. Rev. **84:**623–647.
19. **Pei, Z., G. Liu, T. H. Lubben, and B. G. Szczepankiewicz.** 2004. Inhibition of protein tyrosine phosphatase 1B as a potential treatment of diabetes and obesity. Curr. Pharm. Des. **10:**3481–3504.
20. **Rondinone, C. M., J. M. Trevillyan, J. Clampit, R. J. Gum, C. Berg, P. Kroeger, L. Frost, B. A. Zinker, R. Reilly, R. Ulrich, M. Butler, B. P. Monia, M. R. Jirousek, and J. F. Waring.** 2002. Protein tyrosine phosphatase 1B reduction regulates adiposity and expression of genes involved in lipogenesis. Diabetes **51:**2405–2411.
21. **Shulman, G. I.** 2000. Cellular mechanisms of insulin resistance. J. Clin. Investig. **106:**171–176.
22. **Simoncic, P. D., C. J. McGlade, and M. L. Tremblay.** 2006. PTP1B and TC-PTP: novel roles in immune-cell signaling. Can. J. Physiol. Pharmacol. **84:**667–675.
23. **Taniguchi, C. M., B. Emanuelli, and C. R. Kahn.** 2006. Critical nodes in signalling pathways: insights into insulin action. Nat. Rev. Mol. Cell. Biol. **7:**85–96.
24. **Tonks, N. K.** 2003. PTP1B: from the sidelines to the front lines! FEBS Lett. **546:**140–148.
25. **Waring, J. F., R. Ciurlionis, J. E. Clampit, S. Morgan, R. J. Gum, R. A. Jolly, P. Kroeger, L. Frost, J. Trevillyan, B. A. Zinker, M. Jirousek, R. G. Ulrich, and C. M. Rondinone.** 2003. PTP1B antisense-treated mice show regulation of genes involved in lipogenesis in liver and fat. Mol. Cell. Endocrinol. **203:**155–168.
26. **Wu, Y., J. P. Ouyang, K. Wu, S. S. Wang, C. Y. Wen, and Z. Y. Xia.** 2005. Rosiglitazone ameliorates abnormal expression and activity of protein tyrosine phosphatase 1B in the skeletal muscle of fat-fed, streptozotocin-treated diabetic rats. Br. J. Pharmacol. **146:**234–243.
27. **Zabolotny, J. M., F. G. Haj, Y. B. Kim, H. J. Kim, G. I. Shulman, J. K. Kim, B. G. Neel, and B. B. Kahn.** 2004. Transgenic overexpression of protein-tyrosine phosphatase 1B in muscle causes insulin resistance, but overexpression with leukocyte antigen-related phosphatase does not additively impair insulin action. J. Biol. Chem. **279:**24844–24851.
28. **Zinker, B. A., C. M. Rondinone, J. M. Trevillyan, R. J. Gum, J. E. Clampit, J. F. Waring, N. Xie, D. Wilcox, P. Jacobson, L. Frost, P. E. Kroeger, R. M. Reilly, S. Koterski, T. J. Opgenorth, R. G. Ulrich, S. Crosby, M. Butler, S. F. Murray, R. A. McKay, S. Bhanot, B. P. Monia, and M. R. Jirousek.** 2002. PTP1B antisense oligonucleotide lowers PTP1B protein, normalizes blood glucose, and improves insulin sensitivity in diabetic mice. Proc. Natl. Acad. Sci. USA **99:**11357–11362.
29. **Zisman, A., O. D. Peroni, E. D. Abel, M. D. Michael, F. Mauvais-Jarvis, B. B. Lowell, J. F. Wojtaszewski, M. F. Hirshman, A. Virkamaki, L. J. Goodyear, C. R. Kahn, and B. B. Kahn.** 2000. Targeted disruption of the glucose transporter 4 selectively in muscle causes insulin resistance and glucose intolerance. Nat. Med. **6:**924–928.